Artificial Organs

Artificial Organs
35(8):E174–E180, Wiley Periodicals, Inc.

Thoughts and Progress

A Method for Control of an Implantable Rotary Blood Pump for Heart Failure Patients Using Noninvasive Measurements

**Einly Lim, †Abdul-Hakeem H. Alomari, †Andrey V. Savkin, ‡Socrates Dokos, §John F. Fraser, §Daniel L. Timms, **David G. Mason, and ‡Nigel H. Lovell*
**Department of Biomedical Engineering, Faculty of Engineering, University of Malaya, Kuala Lumpur, Malaysia; †School of Electrical Engineering and Telecommunications and ‡Graduate School of Biomedical Engineering, The University of New South Wales, Sydney, NSW; §Critical Care Research Group, The Prince Charles Hospital; and **Department of Information Technology and Electrical Engineering, The University of Queensland, Brisbane, Queensland, Australia*

Abstract: We propose a deadbeat controller for the control of pulsatile pump flow (Q_p) in an implantable rotary blood pump (IRBP). Noninvasive measurements of pump speed and current are used as inputs to a dynamical model of Q_p estimation, previously developed and verified in our laboratory. The controller was tested using a lumped parameter model of the cardiovascular system (CVS), in combination with the stable dynamical models of Q_p and differential pressure (head) estimation for the IRBP. The control algorithm was tested with both constant and sinusoidal reference Q_p as input to the CVS model. Results showed that the controller was able to track the reference input with minimal error in the presence of model uncertainty. Furthermore, Q_p was shown to settle to the desired reference value within a finite number of sampling periods. Our results also indicated that counterpulsation yields the minimum left ventricular stroke work, left ventricular end diastolic volume, and aortic pulse pressure, without significantly affecting mean cardiac output and aortic pressure. **Key Words:** Implantable rotary blood pump—Deadbeat controller—Pulsatile pump flow.

doi:10.1111/j.1525-1594.2011.01268.x

Received August 2010; revised February 2011.
Address correspondence and reprint requests to Miss Einly Lim, Department of Biomedical Engineering, Faculty of Engineering, University of Malaya, 50603 Kuala Lumpur, Malaysia. E-mail: einly_lim@yahoo.com

Congestive heart failure (CHF) is a health condition characterized by the inability of the heart to supply sufficient blood-borne nutrients to meet the body's metabolic demand. Shortage of donor organs for heart transplantation and limitations in drug therapies have led to a range of treatment alternatives for CHF patients, such as ventricular assist devices (VADs). These include both the pulsatile VADs and the continuous-flow VADs (or implantable rotary blood pumps [IRBPs]). Among these devices, the IRBPs have been increasingly popular due to their smaller size and, therefore, easier implantation.

However, numerous research studies have raised potential concerns regarding their nonphysiological hemodynamics which may lead to alterations in biochemical function (1). A number of clinical advantages of pulsatile perfusion have been hypothesized or proven throughout the years under clinical or animal settings (2,3), mostly during cardiopulmonary bypass procedures. The advantages include less vital organ injury and systemic inflammation (4), beneficial exercising of the aortic valve, higher regional and global myocardial blood flow (leading to increased coronary perfusion), greater degree of left ventricular (LV) pressure and volume unloading (leading to better myocardial recovery) (2), reduced risk of ventricular suction (5), as well as beneficial effects on the vascular properties and microcirculation (6). Despite these reports, few articles have looked into the area of pulsatile flow (Q_p) control of an IRBP. Vandenberghe et al. (7) studied the effect of various pulsatile mode support strategies on pressures and flows in a mock loop, while Korakianitis and Shi (8) performed computer simulations to study the effect of counterpulsation flow control on the hemodynamic response using their mathematical model. Nevertheless, we are not aware of any studies which evaluate the performance of a Q_p controller during transient changes of reference input or model parameters using only noninvasive measurements.

One important design goal of an IRBP is to control the pump without the need for additional implantable sensors. Choi et al. (9) developed a fuzzy logic controller for an axial blood pump based on the blood flow pulsatility, estimated using a validated pump model. On the other hand, Giridharan and

Skliar (10) proposed a model-based method for estimating differential pressure across the pump, which served as the control input for their IRBP. A limitation of the previous work was that the estimation of either Q_p or differential pressure was based on steady-state pump modeling, which had not been validated during transient changes. By accurately estimating the transient response of the pump, one is able to avoid dangerous or undesirable situations caused by sudden perturbations in the cardiovascular system (CVS) during pump operation.

The present article proposes a deadbeat controller for the control of Q_p in the IRBP, using noninvasive measurements of pump speed and current as inputs to a dynamical model of Q_p estimation. A deadbeat controller is a digital controller which drives the system error to zero after a minimum possible sampling period and exhibits no intersampling ripples after the steady state is reached (11). The ability to respond quickly to sudden perturbations in the CVS and adjust Q_p accordingly is highly desirable due to the fact that sudden changes in afterload or preload may cause undesirable effects on the CVS, such as ventricular collapse, if the pump control does not react fast enough. The controller was tested using a lumped parameter model of the CVS (12), in combination with the stable dynamical models of Q_p and differential pressure (head) estimation for the IRBP (13). The models have been developed and validated previously in our laboratory against mock loop data and animal experimental measurements. The control algorithm was tested with both constant and sinusoidal reference Q_p as input to the model.

METHODS

A software model incorporating a lumped parameter model of the CVS in combination with a stable dynamical model of a left VAD (LVAD) was used to evaluate the control strategy.

The software model

The model of the CVS comprised 10 compartments including the left and right sides of the heart, as well as the pulmonary and systemic circulations. Each compartment in the CVS model was formulated based on well-established experimental observations (14). The CVS model parameters were tuned accordingly to reproduce pressure, flow, and volume distributions in a healthy subject (14). A detailed description of the model as well as parameter values, previously developed by our research group, can be obtained from reference (12). The model has been carefully validated using published data from the literature, as well as our animal experiments using healthy pigs implanted with an LVAD. Simulated responses of the model were shown to agree well with the experimental data over a range of pump operating points (12).

In the present article, model parameters reported in reference (12), which correspond to the healthy condition, were used as baseline values for a normal subject. To allow simulation of CHF conditions, general model parameters associated with CHF, including contractility of the left and right ventricle ($E_{es,lv}$ and $E_{es,rv}$), systemic peripheral resistance (R_{sa}), and total blood volume (V_{total}) were modified ($E_{es,lv} = 0.71$ mm Hg/mL; $E_{es,rv} = 0.53$ mm Hg/mL; $R_{sa} = 1.11$ mm Hg/s/mL; $V_{total} = 5800$ mL). These parameters were carefully chosen in order to ensure that realistic simulation, in terms of cardiac output, aortic pressure, and left atrial pressure, was achieved (15).

The LVAD model included the description of the rotary blood pump, as well as the inlet and outlet cannulae. Descriptions of the inlet and outlet cannulae can also be found in reference (12). Stable dynamical models for Q_p and differential pressure estimation of the IRBP using noninvasive measurements of pump power, P, and rotational speed, ω, previously designed and verified using in vivo pig data and in vitro mock loop experimental data by our research group, were used in the present simulation to represent the pump model. Detailed descriptions of the models, including the system identification and validation methods used to obtain them, can be found in reference (13).

In short, a noninvasive, steady-state average flow estimator based on noninvasive measurements of P and ω was developed using data collected in a continuous flow environment. The equation for the steady-state average flow estimator (f) was based on the work of Malagutti et al. (16) and is of the following form:

$$f = a_1 + a_2 P + a_3 P^2 + a_4 P^3 + a_5 \omega + a_6 \omega^2 \qquad (1)$$

where $P = V\ I$ is the product of supply voltage (V) and motor current (I), and a_1-a_6 are functions of viscosity levels (16). f was then used to estimate the Q_p using the dynamical model derived in (13):

$$\begin{aligned} Q_p(k\tau) = {} & 0.2710 f([k-1]\tau) - 0.2546 f([k-2]\tau) - \\ & 1.985 Q_p([k-1]\tau) - 1.240 Q_p([k-2]\tau) - \\ & 0.2397 Q_p([k-3]\tau) + e_1(k\tau) \end{aligned} \qquad (2)$$

Here, τ is the sampling interval equal to 0.02 s and $e_1(k\tau)$ represents the model error. The estimated Q_p, together with the ω, was then used to estimate the

instantaneous differential pressure across the pump (H_p) (13), as defined by

$$\begin{aligned} H_p(k\tau) = {} & -0.476 - 1.157Q_p([k-1]\tau) + \\ & 1.519Q_p([k-2]\tau) - 0.278Q_p([k-3]\tau) - \\ & 0.475Q_p([k-4]\tau) + 0.0683\omega([k-1]\tau) - \\ & 0.0742\omega([k-2]\tau) - 0.0298\omega([k-3]\tau) + \\ & 0.0379\omega([k-4]\tau) - 1.735H_p([k-1]\tau) + \\ & 0.758H_p([k-2]\tau) + e_2(k\tau) \end{aligned} \quad (3)$$

where $e_2(k\tau)$ represents the model error.

The inlet and outlet cannulae formed an important link between the CVS model and the LVAD model. They were each modeled in terms of flow-dependent resistances (R_{in} and R_{out}), as well as inlet and outlet inertias (L_{in} and L_{out}), as follows:

$$\begin{aligned} H_p(t) = {} & H_{cvs}(t) + (R_{in} + R_{out})Q_p^2(t) + \\ & (L_{in} + L_{out})Q_p(t) + e_3(t) \end{aligned} \quad (4)$$

where $H_p(t)$ denotes differential pressure across the pump, $H_{cvs}(t)$ denotes pressure difference between the left ventricle and the aorta, and $e_3(t)$ represents the model error. Parameters for the cannulae model were estimated using data from the in vivo animal experiments (12). Equation 4 was then discretized to obtain a model for the pump differential pressure:

$$\begin{aligned} H_p(k\tau) = {} & H_{cvs}(k\tau) + 1.67Q_p^2(k\tau) + \\ & \frac{0.83}{\tau}(Q_p(k\tau) - Q_p([k-1]\tau)) + e3(k\tau). \end{aligned} \quad (5)$$

Implementation of deadbeat control algorithm

A deadbeat controller algorithm (17) was implemented to control the Q_p, with the Q_p as the control variable. The input to the deadbeat controller is the reference Q_p, estimated Q_p, and estimated differential pressure, while the output of the controller is the pulse with modulation (PWM) voltage signal to the rotary pump, represented as u. ω and P were the only variables measured in our system, and were used to estimate steady-state pump flow, f, using Eq. 1. f was then used to estimate the Q_p and pump differential pressure using Eqs. 2 and 3.

In order to design the control algorithm, we developed a new autoregressive (ARX), with exogenous inputs, model with three input signals describing the relationship between the control output signal, that is, the PWM signal (u), the f, the Q_p, and the pump differential pressure (H_p). The resulting system model is described by the following difference equation:

$$\begin{aligned} f(k\tau) = {} & d_1u([k-3]\tau) + d_2f([k-1]\tau) - d_3f([k-2]\tau) + \\ & d_4Q_p([k-3]\tau) - d_5H_p([k-3]\tau) + e_4(k\tau) \end{aligned} \quad (6)$$

Here, d_1, d_2, d_3, d_4, and d_5 are constants with values of 0.004199, 1.956, –0.962, 0.05766, and –0.0005538, respectively, and $e_4(k\tau)$ represents the model error. Order and parameters of the ARX model which produced the smallest mean absolute error (e) between the estimated and the measured f were chosen. Half of the data from the mock loop experiments described in reference (13) was used to develop the model, while the remaining data were used for model validation.

In the present simulation, two cases were simulated: (i) constant reference input, that is, $r(t) = a$, where a = constant > 0, and (ii) sinusoidal reference input, that is, $r(t) = a + b\sin\left(\frac{2\pi t}{T} + \varphi\right)$, where a, b and ϕ = constants, $a > b$, while T = heart period. In order to achieve the reference value (r) within minimum possible sampling periods, we derived our control output, u, based on Eq. 6:

$$\begin{aligned} u(k\tau) = {} & \frac{1}{d_1}(f([k+3]\tau) - d_2f([k+2]\tau) + \\ & d_3f([k+1]\tau) - d_4Q_p(k\tau) - d_5H_p(k\tau)) \end{aligned} \quad (7)$$

where $\bar{f}$ is the desired f which was derived based on Eq. 2:

$$\begin{aligned} \bar{f}(k\tau) = {} & \frac{1}{0.271}(0.2397Q_p([k-2]\tau) + \\ & 1.240Q_p([k-1]\tau) + 1.985Q_p(k\tau) + \\ & 0.2546f([k-1]\tau) + r([k+1]\tau)) \end{aligned} \quad (8)$$

In all simulations, we added a sinusoidal high-frequency signal at 20 Hz to the model error terms e_1–e_4 in Eqs. 2, 5, and 6 to represent model uncertainty.

Simulation protocols

The model was implemented using the Simulink toolbox in MATLAB (The Mathworks, Inc., Natick, MA, USA). The simulation was first carried out using varying levels of constant reference Q_p input. Next, sinusoidal signals of varying mean, amplitude, and phase shift were applied to the reference Q_p input. Phase shift for the sinusoidal reference Q_p input is defined as 0 when the peak Q_p value occurs during end systole, that is, at the maximum value of the time-varying elastance function (e_v). In all simulations, frequencies of the sinusoidal signals were chosen to be equal to the heart rate.

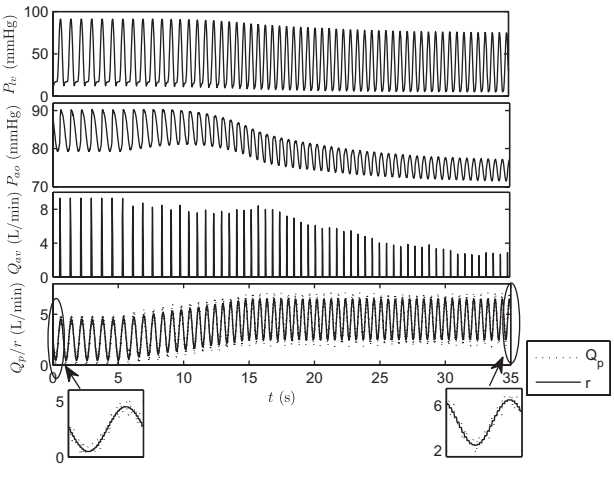

FIG. 1. Left ventricular pressure (P_{lv}), aortic pressure (P_{ao}), pump flow (Q_p), and reference pump flow (r) waveforms from the model simulations using parameters for CHF condition, during transition from rest to exercise. Reference pump flow input (r) was increased linearly from $2.5+2\sin\left(\frac{2\pi t}{T}\right)$ L/min at $t = 15$ *s* to $4.5+2\sin\left(\frac{2\pi t}{T}\right)$ L/min at $t = 15$ *s*.

In order to evaluate the ability of the controller to track the increased reference Q_p input in the presence of model parameter changes, we have simulated transition from rest to exercise. Using model parameters for the CHF condition as baseline values, relevant model parameters associated with exercise were linearly changed over a period of 10 s. These included the R_{sa} (decreased linearly by 50%), unstressed volume of the systemic veins (decreased linearly by 500 mL), and heart rate (increased linearly by 35 bpm). During this period, the reference Q_p signal was increased linearly from $r(t)=2.5+2\sin\left(\frac{2\pi t}{T}\right)$ to $r(t)=4.5+2\sin\left(\frac{2\pi t}{T}\right)$ L/min.

Surplus hemodynamic energy (SHE) was derived from the simulation results as a means of assessing pulsatility (18) defined as

$$SHE\left(\frac{erg}{mL}\right)=1332\left(\frac{\int(Q_p+Q_{av})P_{ao}dt}{\int(Q_p+Q_{av})dt}-\overline{P_{ao}}\right) \quad (9)$$

RESULTS

Figure 1 shows the waveforms of the LV pressure (P_{lv}), aortic pressure (P_{ao}), aortic valve flow (Q_{av}), and Q_p superimposed on the reference Q_p signal (r) generated by the model using parameters for the CHF condition, during transition from rest to exercise. The reference input signal was increased from $r(t)=2.5+2\sin\left(\frac{2\pi t}{T}\right)$ to $r(t)=4.5+2\sin\left(\frac{2\pi t}{T}\right)$ at $t = 5$ s, over an interval of 10 s. The simulated Q_p accurately tracked the reference input signal within an error of ±0.5 L/min. During exercise, both left ventricular end systolic pressure and P_{ao} decreased, while total cardiac output increased.

Figure 2 illustrates the effect of sinusoidal Q_p modulation on end-systolic and end-diastolic LV volume (*Vol*), systolic and diastolic P_{ao}, stroke volume (*SV*), mean cardiac output ($\overline{CO}$), external work (*EW*), *SHE*, and the P_{lv}–volume loops at different phase shifts. The simulation uses parameters for the CHF subject and reference Q_p signal with mean value of 2.5 L/min and amplitude of 2 L/min. Our results indicate that counterpulsation (around 50% phase shift) produced the smallest LV end-diastolic volume, *EW*, *SV*, *SHE*, and aortic pulse pressure. On the contrary, copulsation (0% phase shift) produced the maximum LV stroke work, SHE and LV end-diastolic volume, with the minimum LV end-systolic volume. Despite the large variation in stroke work with different phase shifts, sinusoidal Q_p modulation did not significantly alter $\overline{CO}$ and P_{ao}.

DISCUSSION

Various pump control strategies have been proposed by research groups in the IRBP field. The traditional control strategy, which maintains a constant pump speed, demonstrates a limited degree of adaptability to cardiac demand and pathological state of the heart. In view of this, physiological control algorithms which aim to adjust Q_p according to patients' metabolic demand have been proposed, including pump differential pressure or P_{ao} control (19), flow control (20), and pulsatility index or pulsatility ratio control (21). Schima et al. (20) have reported on the successful implementation of a heart rate-based control strategy in clinical studies. The control system consists of four interacting components, that is, a desired Q_p value based on measured heart rate, a desired peak-to-peak flow value automatically varied by a suction detection unit and two speed variation functions, as well as threshold values for maximal pump power and minimal Q_p. Ochiai et al. (22) proposed an automatic pump control algorithm which maintains a targeted Q_p that is a function of the heart rate to the peak pump inlet–outlet conduit pressure difference (AoP_{calc}) ratio.

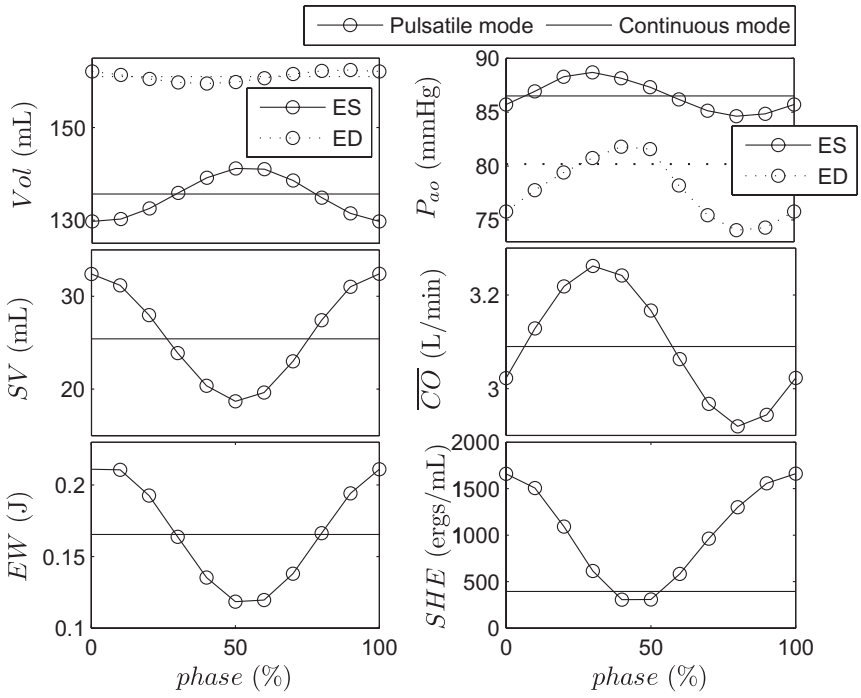

FIG. 2. Effect of sinusoidal Q_p modulation on left ventricular volume (*Vol*; ES, end systolic; ED, end diastolic), aortic pressure (P_{ao}; ES, end systolic; ED, end diastolic), stroke volume (*SV*), mean cardiac output ($\overline{CO}$), external work (*EW*), and surplus hemodynamic energy (*SHE*) at different phase shifts.

Although extensive efforts have been made in the field, Q_p control of an IRBP has not been widely studied, despite potential concerns regarding their nonphysiological hemodynamics as well as the new possibilities it may offer in the field of control. Over the years, pulsatile perfusion has been shown to provide numerous advantages under clinical or animal settings (2,18). These include less vital organ injury and systemic inflammation (4), higher regional and global myocardial blood flow as well as organ perfusion, a greater degree of P_{lv} and volume unloading (2), reduced occurrence of blood stasis in the ventricle, and decreased risk of ventricular suction (5). In view of this, a number of studies (7,23,24) have attempted to generate Q_p in IRBPs or during cardiopulmonary bypass settings. The most commonly used method to achieve this is by varying the voltage on the motor to switch between a low and high rotor speed after a desired mean flow rate is obtained (23). A few important artificial pulse parameters were varied, including beat rate, the minimum and maximum pump speeds, the sharpness of speed changes, and the systolic interval (5). The main drawback of the pulsatile speed control strategy is that it demonstrates a limited degree of adaptability to cardiac demand and pathological state of the heart. As a centrifugal pump is highly afterload dependent, the resultant Q_p does not only depend on ω but varies substantially with changing cardiovascular parameters.

The present study proposed a noninvasive Q_p control strategy (both continuous and pulsatile) based on a stable dynamical model of Q_p estimation, which was able to estimate Q_p during steady-state conditions as well as transient changes in the control input and model parameters (13). The proposed Q_p control algorithm does not stand alone but could form an important part of the multiobjective physiological control algorithm proposed previously by our research group (25). We have chosen to control Q_p instead of pressure, as we believe that Q_p is a more relevant physiological parameter. Furthermore, in a severe heart failure patient, rotary blood Q_p normally contributes completely to total cardiac output; therefore, Q_p is an important parameter which determines total blood flow to the body. In a practical situation, the reference Q_p can be derived from noninvasive indicators of metabolic demand such as heart rate and acceleration (20,25). Our results showed that the controller was able to track the reference input with minimal error in the presence of model uncertainty.

Vandenberghe et al. studied the effect of sinusoidal pump speed variations on the hemodynamic variables, both in the mock loop and computer model (7,24). They found that synchronous pump operation results in maximization of SV and minimization of ventricular pressure, while asynchronous operation causes highly unphysiological pressures and flows.

Our results showed that counterpulsation operation produced the minimum stroke work and LV end-diastolic volume, without significantly affecting the $\overline{CO}$ and P_{ao}. This is highly beneficial for myocardial recovery of a failing heart which operates at its physiological limits of the Frank–Starling relationship, as reduction in stroke work and LV end-diastolic volume decreases myocardial oxygen consumption and LV wall stress (26). It was reported that reducing LV oxygen consumption may attenuate further ischemia of the myocardial tissue and restore the metabolic requirements of reversibly injured myocytes (26). As an added benefit, the relatively higher diastolic P_{ao} during counterpulsation operation may also improve coronary perfusion. Furthermore, using the same mean Q_p input, counterpulsation produced a higher LV end-systolic volume compared to copulsation and continuous operation. This may reduce the risk of ventricular collapse, which is closely related to LV volume during end systole.

Despite the various advantages offered by counterpulsation mode, it has its own drawback in terms of pulsatility. By using pulse pressure and *SHE* for precise pressure-flow waveform quantification, our results showed that copulsation yields a much higher pulsatility compared to counterpulsation. Takeda (27) suggested that the extra energy generated by pulsatility could help to maintain peripheral perfusion by keeping capillary beds open. Having said that, consistent with published findings (28), our results showed that the value for *SHE* generated during copulsation is much lower compared to that generated by a pulsatile pump. Pantalos et al. proposed that for a rotary pump operating in pulsatile mode, an extreme increase in Q_p during systole, which may cause excessive hemolysis and pump wear, would be required to be able to generate the same amount of *SHE* at the same flow rate (28).

Furthermore, the ability of the pump to switch rapidly between low and high rotor pump speeds may be affected by friction that impedes rotation (5). The hydrodynamically suspended pump used in the present study may be suitable for Q_p control because it does not have any friction-producing mechanical bearings. Further work includes evaluation of the control algorithm using a pulsatile mock loop and animal experiments.

CONCLUSION

In this article, we simulated the effect of pump flow modulation on the cardiovascular system in terms of end-systolic and end-diastolic left ventricular volume, systolic and diastolic aortic pressure, stroke volume, mean cardiac output, external work, and surplus hemodynamic energy, at different phase shifts. Counterpulsation is most beneficial for myocardial recovery as it decreases LV EW and oxygen consumption. However, copulsation provides a higher degree of pulsatility compared with counterpulsation control. Furthermore, we examined the performance of a deadbeat controller in the presence of model uncertainty. Results showed that the controller was able to track the reference input with minimal error in the presence of model uncertainty, by using noninvasive measurements. Future work includes testing of the control algorithm using a pulsatile mock loop and evaluating its performance under various physiological conditions such as postural changes and the Valsalva maneuver.

REFERENCES

1. Thalmann M, Schima H, Wiselthaler G, Wolner E. Physiology of continuous blood flow in recipients of rotary cardiac assist devices. *J Heart Lung Transplant* 2005;24:237–45.
2. Klotz S, Deng MC, Stypmann J, et al. Left ventricular pressure and volume unloading during pulsatile versus nonpulsatile left ventricular assist device support. *Ann Thorac Surg* 2004;77: 143–50.
3. Myers G, Undar JL, Rosenberg A. Major factors in the controversy of pulsatile versus nonpulsatile flow during acute and chronic cardiac support. *ASAIO J* 2005;51:173–5.
4. Alkan T, Akcevin A, Undar A, Halil T, Tufan P, Aydn A. Benefits of pulsatile perfusion on vital organ recovery during and after pediatric open heart surgery. *ASAIO J* 2007;53: 651–4.
5. Bourque K, Dague C, Farrar D, et al. In vivo assessment of a rotary left ventricular assist device-induced artificial pulse in the proximal and distal aorta. *Artif Organs* 2006;30:638–42.
6. Hornick K, Taylor P. Pulsatile and nonpulsatile perfusion: the continuing controversy. *J Cardiothorac Vasc Anesth* 1997;11: 310–5.
7. Vandenberghe S, Segers P, Antaki JF, Meyns B, Verdonck PR. Hemodynamic modes of ventricular assist with a rotary blood pump: continuous, pulsatile, and failure. *ASAIO J* 2005;51: 711–8.
8. Korakianitis T, Shi Y. Numerical comparison of hemodynamics with atrium to aorta and ventricular apex to aorta VAD support. *ASAIO J* 2007;53:537–48.
9. Choi S, Antaki JF, Boston JR, Thomas D. A sensorless approach to control of a turbodynamic left ventricular assist system. *IEEE Trans Control Syst Technol* 2001;9:473–82.
10. Giridharan GA, Skliar M. Physiological control of blood pumps using intrinsic pump parameters: a computer simulation study. *Artif Organs* 2006;30:301–7.
11. Ogata K. *Discrete-Time Control Systems*. Englewood Cliffs, NJ: Prentice Hall, 1994.
12. Lim E, Dokos S, Cloherty SL, et al. Parameter-optimized model of cardiovascular-rotary blood pump interactions. *IEEE Trans Biomed Eng* 2010;57:254–66.
13. Alomari AH, Savkin AV, Karantonis DM, Lim E, Lovell NH. Non-invasive estimation of pulsatile flow and differential pressure in an implantable rotary blood pump for heart failure patients. *Physiol Meas* 2009;30:371–86.
14. Guyton AC, Hall JE. *Textbook of Medical Physiology*. Philadelphia, PA: W.B. Saunders Company, 1996.

15. Epstein SE, Beiser GD, Stampfer M, Robinson BF, Braunwald E. Characterization of the circulatory response to maximal upright exercise in normal subjects and patients with heart disease. *Circulation* 1967;35:1049–62.
16. Malagutti N, Karantonis DM, Cloherty SL, et al. Non-invasive average flow estimation for an implantable rotary blood pump: a new algorithm incorporating the role of blood viscosity. *Artif Organs* 2007;31:45–52.
17. Astrom KJ, Wittenmark B. *Computer Controlled Systems*. Reading, MA: Longman Higher Education, 1997.
18. Undar A, Zapanta CM, Reibson JD, et al. Precise quantification of pressure flow waveforms of a pulsatile ventricular assist device. *ASAIO J* 2005;51:56–9.
19. Giridharan G, Pantalos G, Koenig S, Gillars K, Skliar M. Achieving physiologic perfusion with ventricular assist devices: comparison of control strategies. *American Control Conference*. Portland, OR, USA: Proceedings of the 2005 American Control Conference, 2005.
20. Schima H, Vollkron M, Jantsch U, et al. First clinical experience with an automatic control system for rotary blood pumps during ergometry and right-heart catheterization. *J Heart Lung Transplant* 2006;25:167–73.
21. Choi S, Boston JR, Antaki JF. Hemodynamic controller for left ventricular assist device based on pulsatility ratio. *Artif Organs* 2007;31:114–25.
22. Ochiai Y, Golding LAR, Massiello AL, et al. In vivo hemodynamic performance of the Cleveland Clinic CorAide blood pump in calves. *Ann Thorac Surg* 2001;72:747–52.
23. Wang S, Rider AR, Kunselman AR, Richardson JS, Dasse KA, Undar A. Effects of the pulsatile flow settings on pulsatile waveforms and hemodynamic energy in a PediVASTM centrifugal pump. *ASAIO J* 2009;55:271–6.
24. Vandenberghe S, Segers P, Meyns B, Verdonck P. Unloading effect of a rotary blood pump assessed by mathematical modeling. *Artif Organs* 2003;27:1094–101.
25. Karantonis D, Lim E, Mason DG, Salamonsen RF, Ayre PJ, Lovell NH. Non-invasive activity-based control of an implantable rotary blood pump: comparative software simulation study. *Artif Organs* 2010;34:E34–E45.
26. Goldstein AH, Monreal G, Kambara A, et al. Partial support with a centrifugal left ventricular assist device reduces myocardial oxygen consumption in chronic, ischemia heart failure. *J Card Fail* 2005;11:142–51.
27. Takeda J. Experimental study of peripheral circulation during extracorporeal circulation, with a special reference to a comparison of pulsatile flow and non-pulsatile flow. *Arch Jpn Chir* 1960;29:1407–30.
28. Pantalos GM, Giridharan G, Colyer J, et al. Effect of continuous and pulsatile flow left ventricular assist on pulsatility in a pediatric animal model of left ventricular dysfunction: pilot observations. *ASAIO J* 2007;53:385–91.